

Article

Not peer-reviewed version

---

# Machine Learning on Ultrasound Texture Analysis Data for Characterizing of Salivary Glandular Tumors: A Feasibility Study

---

[Li-Jen Liao](#)<sup>\*</sup>, [Ping-Chia Cheng](#), Feng-Tsan Chan

Posted Date: 25 June 2024

doi: 10.20944/preprints202406.1750.v1

Keywords: ultrasound; texture analysis; machine learning



Preprints.org is a free multidiscipline platform providing preprint service that is dedicated to making early versions of research outputs permanently available and citable. Preprints posted at Preprints.org appear in Web of Science, Crossref, Google Scholar, Scilit, Europe PMC.

Copyright: This is an open access article distributed under the Creative Commons Attribution License which permits unrestricted use, distribution, and reproduction in any medium, provided the original work is properly cited.

## Article

# Machine Learning on Ultrasound Texture Analysis Data for Characterizing of Salivary Glandular Tumors: A Feasibility Study

Li-Jen Liao <sup>1,2,3,\*</sup>, Ping-Chia Cheng <sup>1</sup> and Feng-Tsan Chan <sup>4</sup>

<sup>1</sup> Department of Otolaryngology Head and Neck surgery, Far Eastern Memorial Hospital, New Taipei, Taiwan

<sup>2</sup> Biomedical Engineering Office, Far Eastern Memorial Hospital, New Taipei, Taiwan

<sup>3</sup> Department of Electrical Engineering, Yuan Ze University, Taoyuan, Taiwan

<sup>4</sup> Department of Pediatrics, Ten-Chen Hospital, Taoyuan, Taiwan

\* Correspondence: liaolj@ntu.edu.tw; Tel.: 886-2-8966-7000 ext. 1033

**Abstract: Background:** Objective quantitative texture characteristics may be helpful in salivary glandular tumor differential diagnosis. This study uses machine learning (ML) to explore and validate the performance of ultrasound (US) texture features in diagnosing salivary glandular tumors. **Material and methods:** 122 patients with salivary glandular tumors, including 71 benign and 51 malignant tumors, are enrolled. A representative brightness mode US pictures are selected for further Gray Level Co-occurrence Matrix (GLCM) texture analysis. We use t-test to test the significance and use receiver operating characteristic curve method to fund optimal cut-point for these significant features. After splitting 80% data into training set and 20% data into testing set, we use five machine learning models k-nearest Neighbors (kNN), Naïve Bayes, Logistic regression, Artificial Neural Networks (ANN) and supportive vector machine (SVM) to explore and validate the performance of US GLCM texture features in diagnosing salivary glandular tumors. **Results:** This study includes 49 female and 73 male patients, with a mean age of 53 years old, ranging from 21 to 93. We find that six GLCM texture features (contrast, inverse difference movement, entropy, dissimilarity, inverse difference and difference entropy) are significantly different between benign from malignant tumors ( $p < 0.05$ ). On ML, the overall accuracy rates are 74.3% (95%CI: 59.8-88.8%), 94.3% (86.6-100%), 72% (54-89%), 84% (69.5-97.3%) and 73.5% (58.7-88.4%) for kNN, Naïve Bayes, Logistic regression, one node ANN and SVM, respectively. **Conclusion:** US texture analysis with ML has potential as an objective and valuable tool for assessment of salivary gland tumors.

**Keywords:** ultrasound; texture analysis; machine learning

## 1. Introduction

Salivary gland tumor is difficult to have a definite diagnosis before surgical intervention [1]. Computer tomography, Magnetic Resonance Imaging and ultrasound (US) are commonly used to detect the salivary gland tumors. Due to without radiation exposure, point-of-care use and real-time feature, US could be used as the first-line tool to check salivary gland tumors [2–4]. Besides, US can be used to real-time guiding fine needle biopsy, although the diagnostic rate is reported only around sixty percent [5]. Even with US guiding, core needle biopsy still has false negative and false positive diagnosis[6]. Therefore, the definite diagnosis is usually still depended on surgical pathology.

High resolution US is widely used in the preoperative evaluation for salivary tumors[7]. Previous studies reported several subjective US features are related to malignancy, such as calcification, loss of posterior enhancement, poor defined margin and accompanied cervical lymphadenopathy[8]. However, evaluation with US is still limited as a subjective and operator dependent diagnostic technique.

Quantitative texture analysis of US picture provides a more subjective assessment and is hopeful in reducing operator variations[9]. US texture analysis had been ever applied for differentiate preterm from term fetal lungs[10], thyroid nodules[11] and chronic radiation-induced sialoadenitis[12].

Machine learning (ML) is an application of artificial intelligence, which can learn from the data and may improve predictive outcomes by using the data[13]. Image classification is an important application for ML including the US pictures.

Objective quantitative texture characteristics may be helpful in salivary glandular tumor differential diagnosis. Previous study ever reported texture features, including entropy and contrast were can different benign from malignant salivary tumors[14]. However, no previous study used ML to access the diagnostic performance of US texture features in diagnosing salivary glandular tumors. Thus, this study aims to use ML to explore and validate the feasibility of US texture features in diagnosing salivary glandular tumors.

## 2. Materials and Methods

A general overview for this study is illustrated in Figure 1.

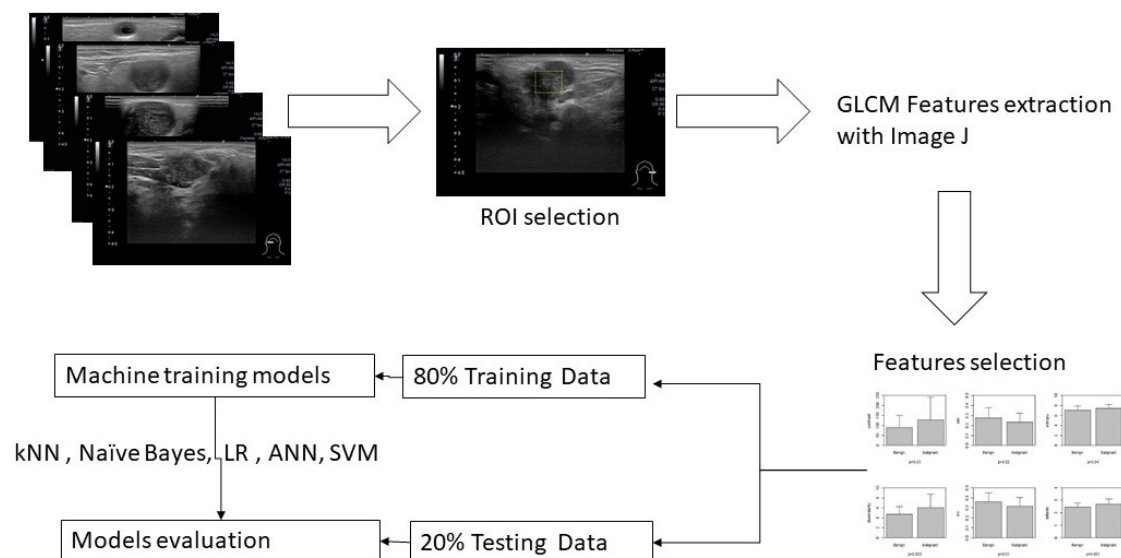


**Figure 1.** Overview of the workflow for this study.

A representative brightness mode US pictures are selected for each patient (Figure 2). Maximal rectangle area within the salivary glandular tumor are delineated for Gray Level Co-occurrence Matrix (GLCM) texture analysis. We calculate eighteen texture features including angular second moment (asm), contrast, correlation, inverse difference moment (IDM), entropy, dissimilarity, inverse difference (INV), variance, cluster shade(CS), Cluster prominence (CP), maximal prominence (maxpro), sum average (sumavg), sum entropy (sumenth), sum variance (sumvar), difference variance (diffvar) and difference entropy (Diffenth) and sum the average for 0, 45, 90 and 135 degree for further comparisons[9,11,12]. We use t-test to check the significance among different texture features., the select the significant predictors for further diagnostic performance assessment with ML models. After splitting 80% data into training set and 20% into testing set, we use five machine learning models k-nearest Neighbors (kNN), Naïve Bayes, Logistic regression, Artificial Neural Networks (ANN) and supportive vector machine (SVM) to explore and validate the performance of US GLCM texture features in diagnosing salivary glandular tumors[15]. In kNN and Naïve Bayes models, the values are normalized as subtract the minimum value and divide by the range. In logistic regression, we further use ROC method to fund optimal cut-point for these significant features and split the data into category with the cut points. In ANN and SVM the raw data are taken into modeling.

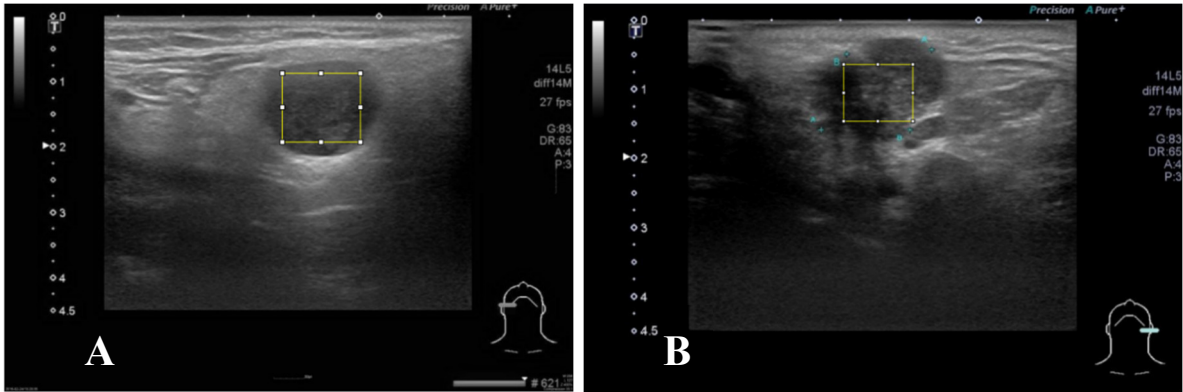


**Figure 2.** (A) case 2 The square block is sampled from a right parotid tumor for GLCM texture analysis by Image J. The pathologic report reveals pleomorphic adenoma. (B) The square block is sampled for GLCM texture analysis from another left parotid tumor, the pathologic report reveals mucoepidermoid carcinoma.

The GLCM texture analysis is done by Image J[16]. All statistical analyses & ML are performed by using STATA 12.0 (Stata Corp Texas 77845 USA) and R version 4.1.0[17].

3. Results

Total 122 patients with salivary glandular tumors, including 71 benign and 51 malignant tumors, are enrolled. There are 49 female and 73 male patients, with a mean age of 53 years old, ranging from 21 to 93. The general characteristics of recruited patients is summarized in Table 1. There are six features different benign from malignancy including contrast ( $90.2\pm58.0$  versus  $129.2\pm115.4$ , p-value =0.03), IDM ( $0.28\pm0.10$  versus  $0.23\pm0.09$ , p-value =0.02), entropy ( $7.01\pm0.87$  versus  $7.39\pm0.86$ , p-value =0.04), dissimilarity ( $4.70\pm1.53$  versus  $6.08\pm2.72$ , p-value =0.002), INV ( $0.36\pm0.09$  versus  $0.32\pm0.09$ , p-value =0.01 ), and Diffenth (  $2.47\pm0.31$  versus  $2.7\pm0.41$ , p-value =0.0006).

**Table 1.** Demographic and texture analysis results of recruited patients.

Characteristics	Benign	Malignant	p-value
Age	50.5±12.8	56.1±17.8	0.06
Gender (F/M)	30/41	19/32	0.71
Size-short axis	1.58±0.59	1.79±0.60	0.06
Size-long axis	2.35±0.95	2.51±0.91	0.35
Contrast	90.2±58.0	129.2±115.4	0.03
IDM	0.28±0.10	0.23±0.09	0.02
Entropy	7.01±0.87	7.39±0.86	0.04
Dissimilarity	4.70±1.53	6.08±2.72	0.002
INV	0.36±0.09	0.32±0.09	0.01
Diffenth	2.47±0.31	2.7±0.41	0.0006
Final diagnosis	Pleomorphic adenoma (29) Warthin's tumor (24) Chronic sialadenitis (5) Basal cell adenoma (4) Lymphoepithelial cyst (2) Nodular fasciitis (2) Benign cyst(2) Epidermal cyst(1) Lipoma(1) Reactive hyperplasia LN(1)	Metastatic carcinoma(26) Invasive carcinoma(6) Mucoepidermoid carcinoma(3) Acinic cell carcinoma(3) Lymphoepithelial carcinoma(2) Adenoid cystic carcinoma(2) Carcinoma ex-pleomorphic adenoma(2) Adenocarcinoma(1) Diffuse large B cell lymphoma(1) High-grade B cell lymphoma(1)	

Blue round cell tumor(1)  
Lymphoblastic lymphoma(1)  
Squamous cell carcinoma(1)  
Salivary ductal carcinoma(1)

Abbreviations: IDM, inverse difference moment; INV, inverse difference; Diffenth, difference entropy; LN, lymph node.

On machine learning, the overall accuracy rates are 74.3% (95%CI:59.8-88.8%), 94.3%(86.6-100%), 72%(54-89%), 84%(69.5-97.3%) and 73.5% (58.7-88.4%) for kNN, Naïve Bayes, Logistic regression, one node ANN (Figure 3) and SVM, respectively. Detail diagnostic performances including sensitivity and specificity are summarized in Table 2.

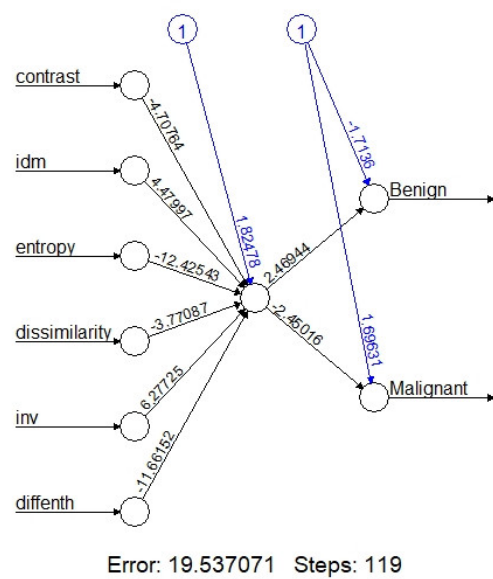


**Figure 3.** With one hidden node with 6 predictors, the accurate rate of this ANN model is 84.0 % (95% CI: 69.5-97.3%).

**Table 2.** This is a table. Tables should be placed in the main text near to the first time they are cited.

	Sensitivity	Specificity	Overall Accuracy
kNN (k=5)	62.5(38.8-86.2)%	84.2(67.8-100)%	74.3(59.8-88.8)%
naïve Bay	88.2(72.9-100)%	100%	94.3(86.6-100)%
Logistic regression	75.0(32.6-100)%	71.4(52.1-90.8)%	72.0(54.4-89.6)%
ANN	60.0(29.6-90.4)%	100%	84.0(69.5-97.3)%
SVM	87.5(64.6-100)%	69.2(51.5-87.0)%	73.5(58.7-88.4)%

Abbreviations: kNN, k-nearest Neighbors; ANN, Artificial Neural Networks; SVM, Supportive vector machine.

4. Discussion

This is the first study used ML to modeling the texture features for salivary glandular tumor. Our result reveals US texture analysis with ML has potential as an objective and valuable tool for assessment of the salivary gland tumors.

Dissimilarity, entropy and contrast related to the heterogeneous content of tumor. Previous study ever reported texture features, including entropy and contrast were can different benign from malignant salivary tumors[14]. In our study, we also find entropy and contrast are also different benign from malignant tumors. Entropy is a quantitative measure of signal uncertainty and has been widely applied to ultrasound tissue characterization. These results mean that the malignant tumors are more heterogeneous and diverse than those in benign tumors.

We also include other four texture features, includes inverse difference moment, dissimilarity, inverse difference and difference entropy for ML. Inverse difference moment (IDM) is usually called



homogeneity that measures the local homogeneity of an image. IDM feature obtains the measures of the closeness of the distribution of the GLCM elements to the GLCM diagonal. In our study, IDM is higher for benign than malignancy ( $0.28 \pm 0.10$  versus  $0.23 \pm 0.09$ ,  $p$ -value = 0.02).

After combinations of these six texture features, the diagnostic performance are 74.3% (95%CI: 59.8-88.8%), 94.3% (86.6-100%), 72% (54-89%), 84% (69.5-97.3%) and 73.5% (58.7-88.4%) for kNN, Naïve Bayes, Logistic regression, one node ANN (Figure 3) and SVM, respectively (Table 2). Although the performance is not perfect. Our results still support that the use of texture analysis may provide objective and quantitative information about the image pattern. Adaptation of more objective features may further increase the diagnostic performance. Computer-aided diagnostic (CAD) system for thyroid nodule sonographic evaluation is successfully developed to assess the thyroid nodules[18,19], in our opinion, objective US CAD for salivary is very promising to established with ML in the future.

Artificial intelligence is attempting to get a computer system to imitate human behavior. ML is a subset of AI technique that attempt to apply statistical models and learning from data. ML is a field within computer science, it differs from traditional computational approaches. In traditional computing, algorithms are sets of explicitly programmed instructions used by computers to calculate or problem solve. ML algorithms instead allow for computers to train on data inputs and use statistical analysis in order to output values that fall within a specific range. Because of this, ML facilitates computers in building models from sample data in order to automate decision-making processes based on data inputs[20].

Two of the most widely adopted ML methods are supervised learning which trains algorithms based on data that is labeled by humans, and unsupervised learning which provides the algorithm with no labeled data in order to allow it to find structure within its input data. This study adapts supervised learning including kNN, Naïve Bayes, Logistic regression, ANN and SVM.

ANN is used to develop ML systems that are based on a biological model of the brain, specifically the bioelectrical activity of the neurons in the brain. Neural works is also called as deep learning. An ANN architecture for a supervised learning could include a layer of multiple input elements, one or more hidden processing layers, and weighted connections between nodes in adjacent layers[20]. Evaluation of an ANN model (Figure 3) in our study shows that the one node ANN model is able to correctly classify the tumor with 84.0 % accuracy rate. Due to limited data, we adapted the simple one node ANN model; more data with multiple nodes and layers may further improve the accuracy rate.

There are some limitations in this study, first: the cases number is still limited. Because this is the preliminary feasibility study, more data is need to consolidation of our findings. Second: other texture analysis methods, such as local binary pattern & multiscale features[21,22] could be used to increase the data. Third, there are other form of US picture, such as Doppler and elastography models also could be adapted in the future study. Fourth, there are more ML algorithms could be used[23].

## 5. Conclusions

US texture analysis with machine learning has potential as an objective and valuable tool for assessment of salivary gland tumors.

**Author Contributions:** Conceptualization, L-J L and F-T C.; methodology, L-J L.; software, L-J L and P-C C.; validation, L-J L and F-T C.; formal analysis, L-J L and P-C C.; investigation, L-J L and P-C C.; resources, L-J L and P-C C.; data curation, L-J L and P-C C.; writing—original draft preparation, L-J L.; writing—review and editing, P-C C.; visualization, L-J L.; supervision, F-T C.; project administration, L-J L.; funding acquisition, L-J L. All authors have read and agreed to the published version of the manuscript.

**Funding:** This work was supported by grants from the Far Eastern Memorial Hospital (FEMH-2024-C-025).

**Institutional Review Board Statement:** The study was conducted in accordance with the Declaration of Helsinki, and ap-proved by the Institutional Ethics review board of Far Eastern Memorial Hospital (IRB:112136-E).

**Informed Consent Statement:** Not applicable.

**Data Availability Statement:** Not available due to privacy and ethical reason.

**Conflicts of Interest:** The authors declare that no conflicts of interest exist.

## References

1. Kuan, E.C.; Mallen-St Clair, J.; St John, M.A. Evaluation of Parotid Lesions *Otolaryngol Clin North Am* **2016**, *49*, 313–325.doi:https://doi.org/10.1016/j.otc.2015.10.004.
2. Bozzato, A.; Zenk J Fau - Greess, H.; Greess H Fau - Hornung, J.; Hornung J Fau - Gottwald, F.; Gottwald F Fau - Rabe, C.; Rabe C Fau - Iro, H.; Iro, H. Potential of ultrasound diagnosis for parotid tumors: analysis of qualitative and quantitative parameters *Otolaryngol Head Neck Surg* **2007**, *137*, 642–646.doi:https://doi.org/10.1016/j.otohns.2007.05.062.
3. Haidar, Y.M.; Moshtaghi, O.; Mahmoodi, A.; Helmy, M.; Goddard, J.A.; Armstrong, W.B. The Utility of In-Office Ultrasound in the Diagnosis of Parotid Lesions *Otolaryngol Head Neck Surg* **2017**, *156*, 511–517.doi:https://doi.org/10.1177/0194599816687744.
4. Liao, L.J.; Wen, M.H.; Yang, T.L. Point-of-care ultrasound in otolaryngology and head and neck surgery: A prospective survey study *J Formos Med Assoc* **2021**, *120*, 1547–1553.doi:https://doi.org/10.1016/j.jfma.2021.02.021.
5. Kovacević, D.O.; Fabijanić, I. Sonographic diagnosis of parotid gland lesions: correlation with the results of sonographically guided fine-needle aspiration biopsy *J Clin Ultrasound* **2010**, *38*, 294–298.doi:https://doi.org/10.1002/jcu.20704.
6. Song, I.H.; Song, J.S.; Sung, C.O.; Roh, J.L.; Choi, S.H.; Nam, S.Y.; Kim, S.Y.; Lee, J.H.; Baek, J.H.; Cho, K.J. Accuracy of Core Needle Biopsy Versus Fine Needle Aspiration Cytology for Diagnosing Salivary Gland Tumors *J Pathol Transl Med* **2015**, *49*,
7. Cheng, P.C.; Chang, C.M.; Huang, C.C.; Lo, W.C.; Huang, T.W.; Cheng, P.W.; Liao, L.J. The diagnostic performance of ultrasonography and computerized tomography in differentiating superficial from deep lobe parotid tumours *Clin Otolaryngol* **2019**, *44*.doi:https://doi.org/10.1111/coa.13289.
8. Lo, W.A.-O.; Chang, C.M.; Wang, C.T.; Cheng, P.W.; Liao, L.A.-O. A Novel Sonographic Scoring Model in the Prediction of Major Salivary Gland Tumors *Laryngoscope* **2021**, *131*, E157–E162.doi:https://doi.org/10.1002/lary.28591.
9. Haralick, R.M.; Shanmugam, K.; Dinstein, I.H. Textural features for image classification *IEEE Transactions on systems, man, and cybernetics* **1973**, 610–621
10. Ghorayeb, S.R.; Bracero, L.A.; Blitz, M.J.; Rahman, Z.; Lesser, M.L. Quantitative Ultrasound Texture Analysis for Differentiating Preterm From Term Fetal Lungs *J Ultrasound Med* **2017**, *36*, 1437–1443
11. Bhatia, K.S.; Lam, A.C.; Pang, S.W.; Wang, D.; Ahuja, A.T. Feasibility Study of Texture Analysis Using Ultrasound Shear Wave Elastography to Predict Malignancy in Thyroid Nodules *Ultrasound Med Biol* **2016**, *42*, 1671–1680.doi:https://doi.org/10.1016/j.ultrasmedbio.2016.01.013.
12. Yang, X.; Tridandapani S Fau - Beitler, J.J.; Beitler Jj Fau - Yu, D.S.; Yu Ds Fau - Yoshida, E.J.; Yoshida Ej Fau - Curran, W.J.; Curran Wj Fau - Liu, T.; Liu, T. Ultrasound GLCM texture analysis of radiation-induced parotid-gland injury in head-and-neck cancer radiotherapy: an in vivo study of late toxicity *Med Phys* **2012**, *39*, 5732–5739.doi:https://doi.org/10.1118/1.4747526.
13. Brattain, L.J.; Telfer, B.A.; Dhyani, M.; Grajo, J.R.; Samir, A.E. Machine learning for medical ultrasound: status, methods, and future opportunities *Abdom Radiol (NY)* **2018**, *43*, 786–799.doi:https://doi.org/10.1007/s00261-018-1517-0.
14. Yonetsu, K.; Ohki M Fau - Kumazawa, S.; Kumazawa S Fau - Eida, S.; Eida S Fau - Sumi, M.; Sumi M Fau - Nakamura, T.; Nakamura, T. Parotid tumors: differentiation of benign and malignant tumors with quantitative sonographic analyses *Ultrasound Med Biol* **2004**, *30*, 567–574.doi:https://doi.org/10.1016/j.ultrasmedbio.2004.02.007.
15. Lantz, B., Machine learning with R: expert techniques for predictive modeling, Packt publishing ltd2019.
16. Schneider, C.A.; Rasband Ws Fau - Eliceiri, K.W.; Eliceiri, K.W. NIH Image to ImageJ: 25 years of image analysis *Nat Methods* **2012**, *9*.doi:https://doi.org/10.1038/nmeth.2089.
17. Team, R.C. R: A language and environment for statistical computing. R Foundation for Statistical Computing (No Title) **2013**,
18. Chi, J.; Walia, E.; Babyn, P.; Wang, J.; Groot, G.; Eramian, M. Thyroid Nodule Classification in Ultrasound Images by Fine-Tuning Deep Convolutional Neural Network *J Digit Imaging* **2017**, *30*, 477–486.doi:https://doi.org/10.1007/s10278-017-9997-y.
19. Chai, Y.J.; Song, J.; Shaeer, M.; Yi, K.H. Artificial intelligence for thyroid nodule ultrasound image analysis *Annals of Thyroid* **2020**, *5*.doi:http://dx.doi.org/10.21037/a.
20. Nwanganga, F.; Chapple, M., Practical machine learning in R, John Wiley & Sons2020.
21. Nanni, L.; Lumini A Fau - Brahnam, S.; Brahnam, S. Local binary patterns variants as texture descriptors for medical image analysis *Artif Intell Med* **2010**, *49*, 117–125.doi:https://doi.org/10.1016/j.artmed.2010.02.006.

22. Materka, A.; Strzelecki, M. Texture analysis methods—a review *Technical university of lodz, institute of electronics, COST B11 report, Brussels* **1998**, 10, 4968
23. Uddin, S.A.-O.; Khan, A.; Hossain, M.E.; Moni, M.A. Comparing different supervised machine learning algorithms for disease prediction *BMC Med Inform Decis Mak* **2019**, 19, 281.doi:<https://doi.org/10.1186/s12911-019-1004-8>.

**Disclaimer/Publisher's Note:** The statements, opinions and data contained in all publications are solely those of the individual author(s) and contributor(s) and not of MDPI and/or the editor(s). MDPI and/or the editor(s) disclaim responsibility for any injury to people or property resulting from any ideas, methods, instructions or products referred to in the content.